

Article

# Transport in a Bare Loam Soil Using Lysimeters and Field Plots

Arnaud Isch <sup>1,\*</sup>, Denis Montenach <sup>2</sup>, Frederic Hammel <sup>2</sup>, Philippe Ackerer <sup>3</sup> and Yves Coquet <sup>4,\*</sup>

<sup>1</sup> UMR 7327 ISTO, Centre national de la recherche scientifique (CNRS), Université d'Orléans, 45071 Orleans, France

<sup>2</sup> UE SEAV, Institut national de la recherche agronomique (INRA), 68021 Colmar, France; denis.montenach@inra.fr (D.M.); frederic.hammel@inra.fr (F.H.)

<sup>3</sup> LHyGeS, Université de Strasbourg/EOST—CNRS, 67000 Strasbourg, France; ackerer@unistra.fr

<sup>4</sup> UMR 1402 ECOSYS, AgroParisTech, INRA, 78850 Thiverval-Grignon, France

\* Correspondence: arnaud.isch@cnrs-orleans.fr (A.I.); yves.coquet@agroparistech.fr (Y.C.)

Received: 3 May 2019; Accepted: 3 June 2019; Published: date

**Abstract:** The purpose of this methodological study was to test whether similar soil hydraulic and solute transport properties could be estimated from field plots and lysimeter measurements. The transport of water and bromide (as an inert conservative solute tracer) in three bare field plots and in six bare soil lysimeters were compared. Daily readings of matric head and volumetric water content in the lysimeters showed a profile that was increasingly humid with depth. The hydrodynamic parameters optimized with HYDRUS-1D provided an accurate description of the experimental data for both the field plots and the lysimeters. However, bromide transport in the lysimeters was influenced by preferential transport, which required the use of the mobile/immobile water (MIM) model to suitably describe the experimental data. Water and solute transport observed in the field plots was not accurately described when using parameters optimized with lysimeter data (cross-simulation), and vice versa. The soil's return to atmospheric pressure at the bottom of the lysimeter and differences in tillage practices between the two set-ups had a strong impact on soil water dynamics. The preferential flow of bromide observed in the lysimeters prevented an accurate simulation of solute transport in field plots using the mean optimized parameters on lysimeters and vice versa.

**Keywords:** field plots; lysimeters; optimization; inverse method; hydrodynamic parameters; cross simulations

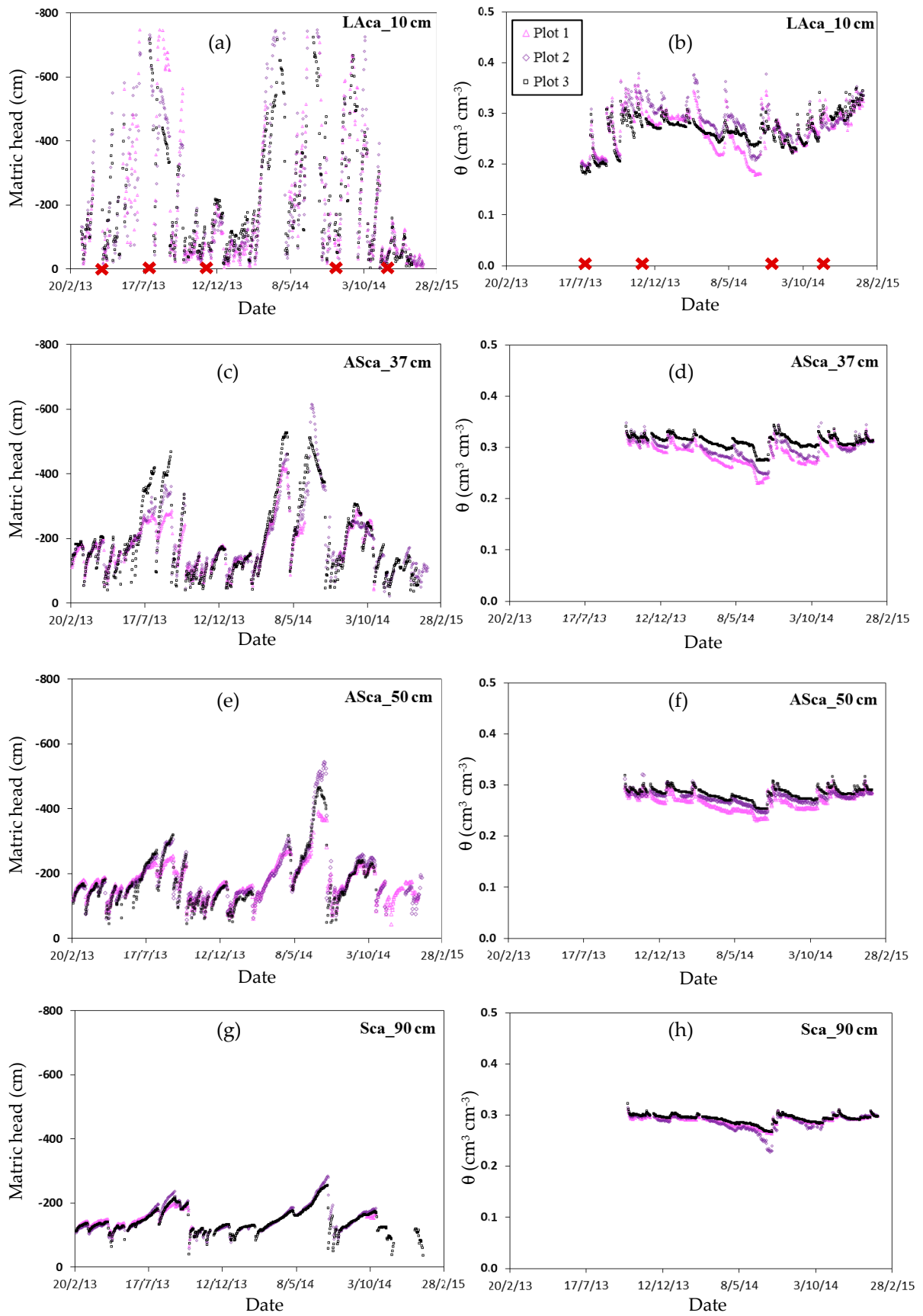


**Figure S1.** Evolution of daily matric head and volumetric water content data measured at the 10 ((a); (b)), 37 ((c); (d)), 50 ((e); (f)) and 90 ((g); (h)) cm depths in the three field plots.

Note: The red crosses indicate the dates on which the instruments in the LAcA horizon (0–28 cm) were put back in place after tillage.

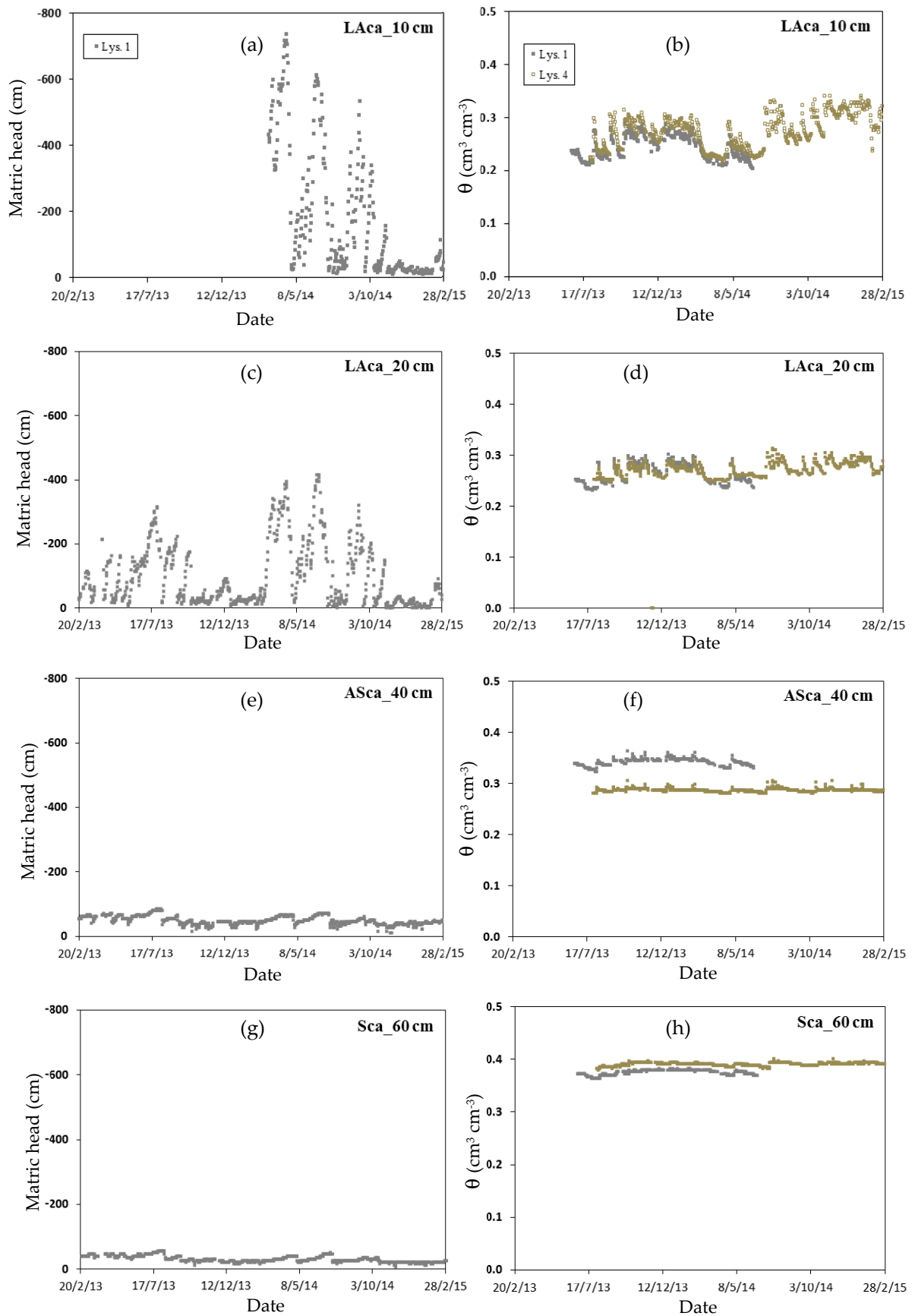


**Figure S2.** Evolution of daily matric head and water content data measured at the 10 ((a); (b)), 20 ((c); (d)), 40 ((e); (f)) and 60 ((g); (h)) cm depths in Lys. 1 and 4.

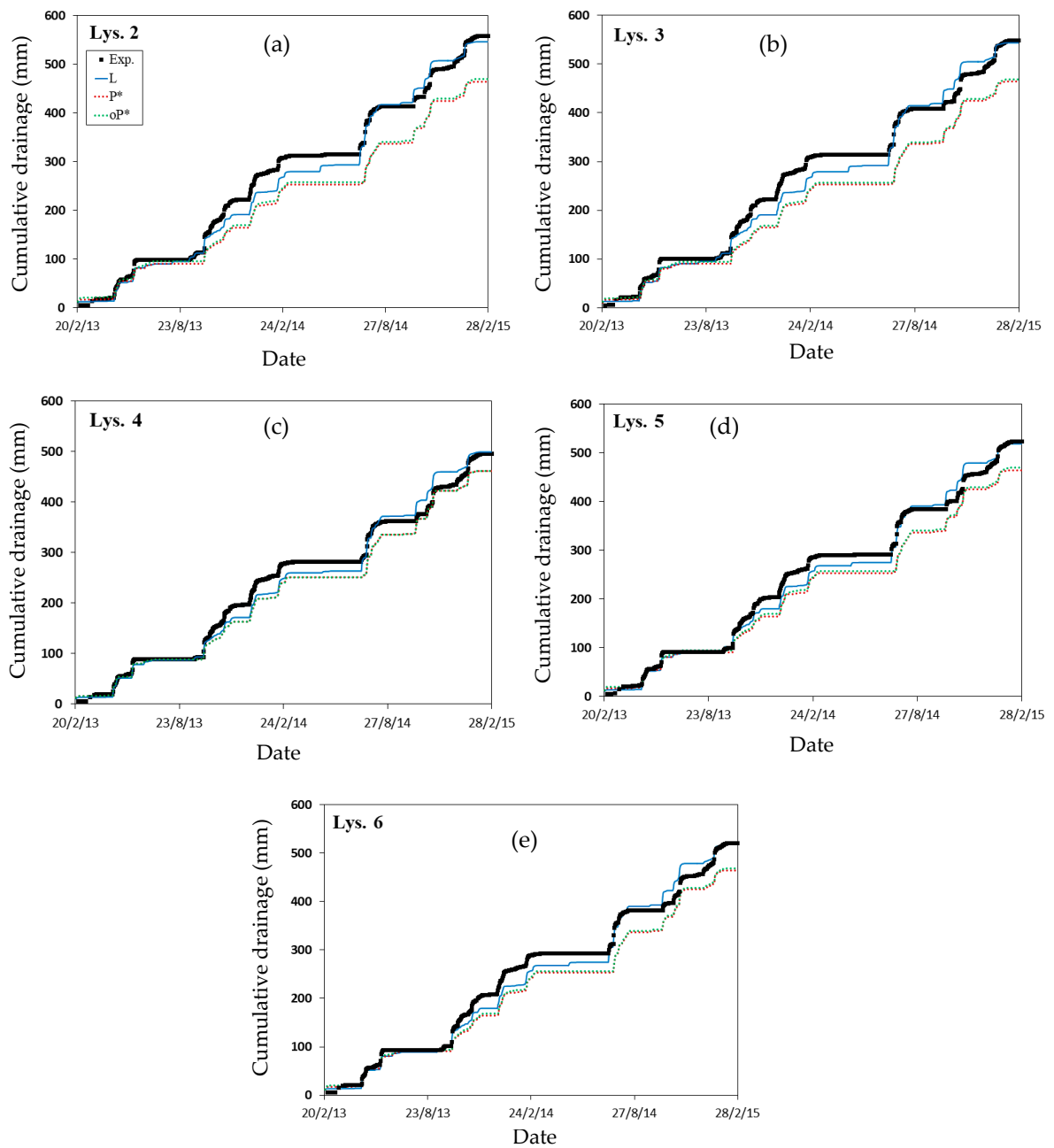


**Figure S3.** Comparison between experimental and simulated drainage on Lys. 2 (a), 3 (b), 4 (c), 5 (d) and 6 (e).

Note: L for results obtained with optimized parameters with HYDRUS-1D on lysimeter data; P\* for results obtained by applying the mean optimized parameters from the 165 cm deep profile of the three field plots; oP\*, the same as P\* but for saturated water content values ( $\theta_s^*$ ) again optimized for each soil material.

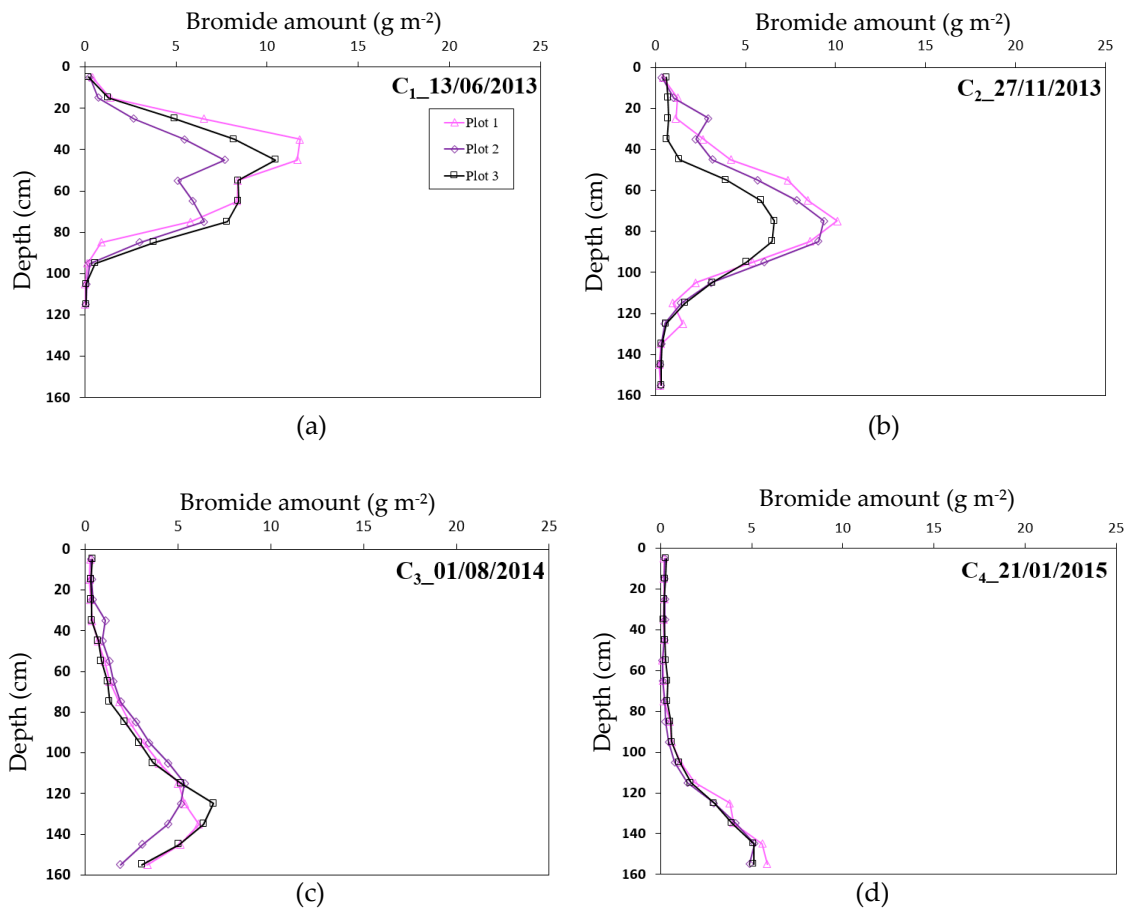


**Figure S4.** The average bromide concentration profiles obtained for each of the four monitoring campaigns (C<sub>1</sub> (a), C<sub>2</sub> (b), C<sub>3</sub> (c), and C<sub>4</sub> (d)).

Note: To facilitate comparison of the results obtained on each field plot, the standard deviations are not shown on the curves. Due to problems with the Geonor sampler for C<sub>4</sub> on Plot 1, only data obtained from the samples taken with the auger were accounted for.

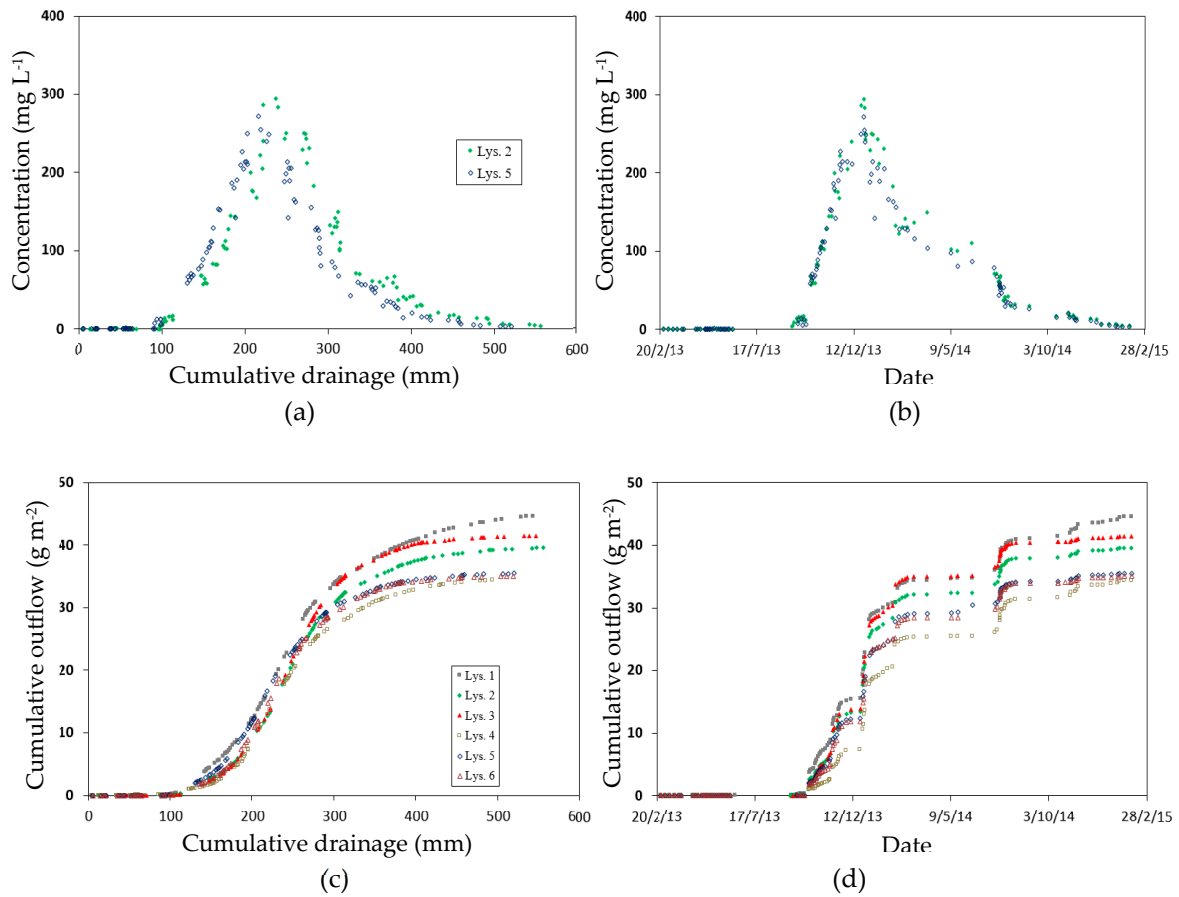


**Figure S5.** Bromide concentration (Lys. 2 and 5) and cumulative outflow (all lysimeters), as a function of cumulative drainage ((a); (c)) and time ((b); (d)).

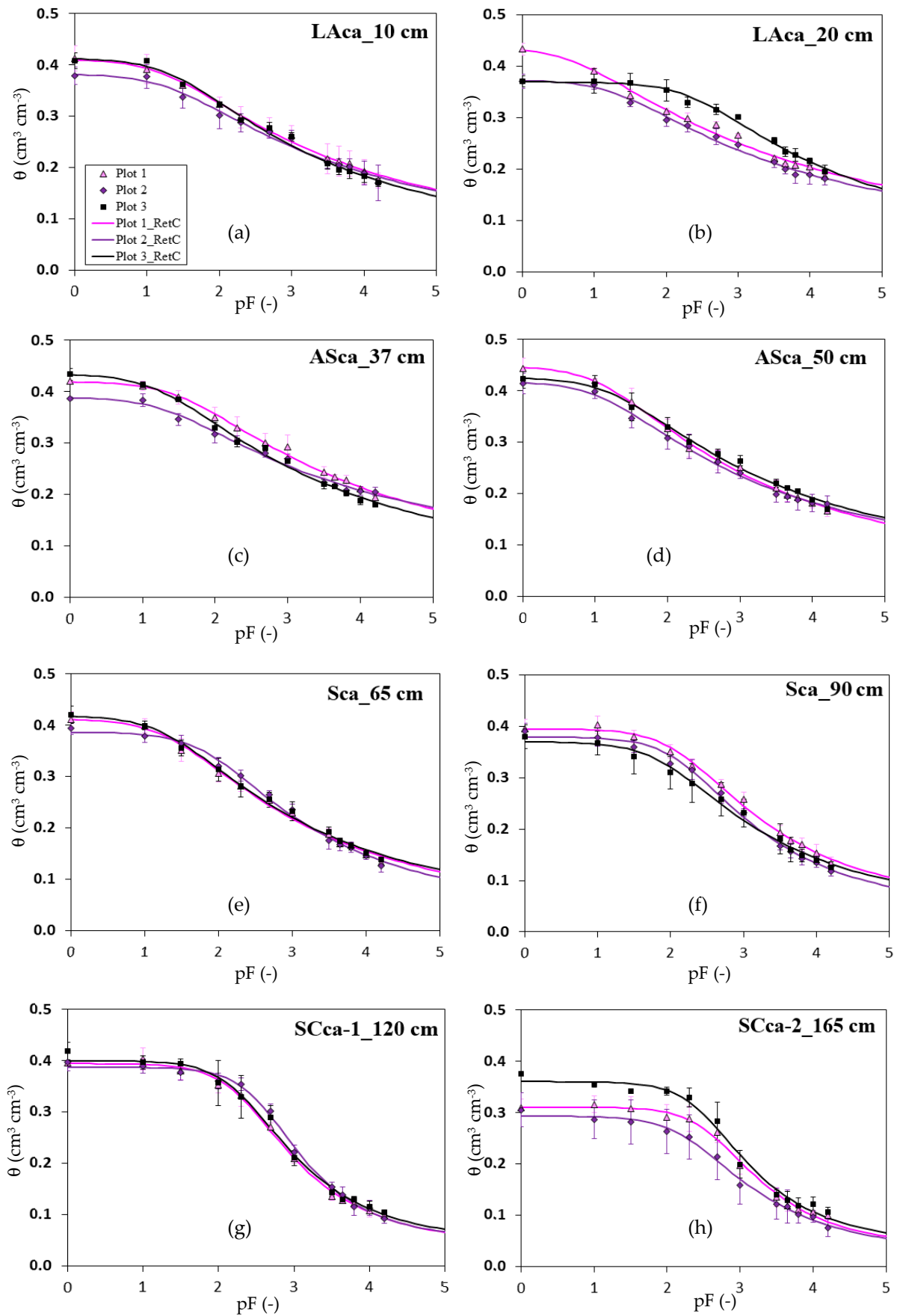


**Figure S6.** Comparison between experimental (obtained in the laboratory) and fitted (with RetC) water retention curves at the 10 (a), 20 (b), 37 (c), 50 (d), 65 (e), 90 (f), 120 (g) and 165 (h) cm depths on the three field plots.

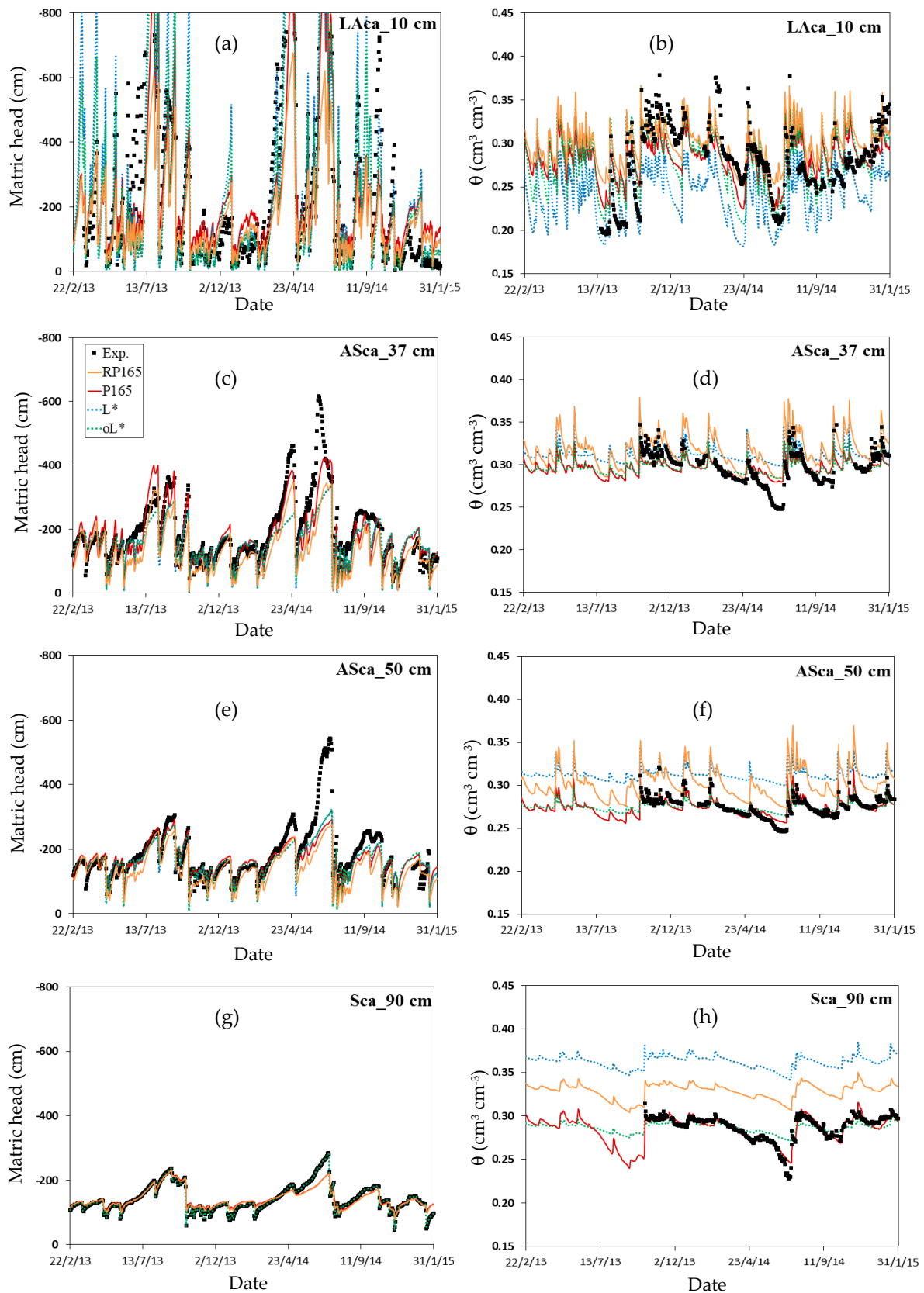


**Figure S7.** Comparison of experimental and simulated matric head and volumetric water content data at the 10 ((a); (b)), 37 ((c); (d)), 50 ((e); (f)) and 90 ((g); (h)) cm depths on Field Plot 2.

Note: RP165 for results obtained with the parameters optimized with RetC, P165 for results obtained with the parameters optimized with HYDRUS-1D on the 165 cm deep profile; P90 for results obtained by applying the parameters optimized for the 165 cm deep profile to the 90 cm deep profile; L\* for results obtained by applying the mean optimized parameters from the six lysimeters; oL\*, the same as L\* but for saturated water content values ( $\theta_s^*$ ) again optimized for each soil material.



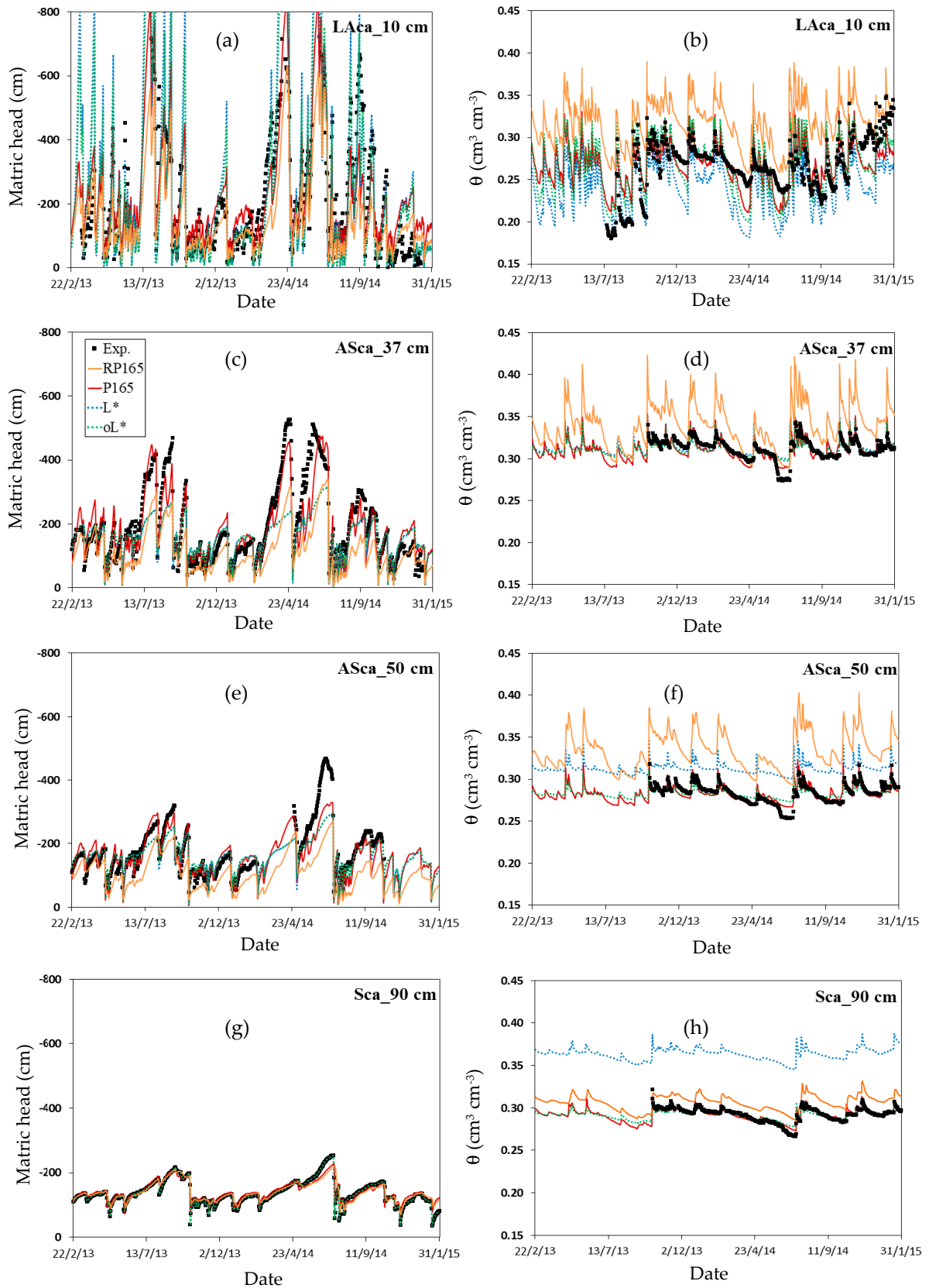


**Figure S7 (continued).** Comparison of experimental and simulated matric head and volumetric water content data at the 10 ((a); (b)), 37 ((c); (d)), 50 ((e); (f)) and 90 ((g); (h)) cm depths on Field Plot 3.

Note: RP165 for results obtained with the parameters optimized with RetC, P165 for results obtained with the parameters optimized with HYDRUS-1D on the 165 cm deep profile; P90 for results obtained by applying the parameters optimized for the 165 cm deep profile to the 90 cm deep profile; L\* for results obtained by applying the mean optimized parameters from the six lysimeters; oL\*, the same as L\* but for saturated water content values ( $\theta_s^*$ ) again optimized for each soil material.

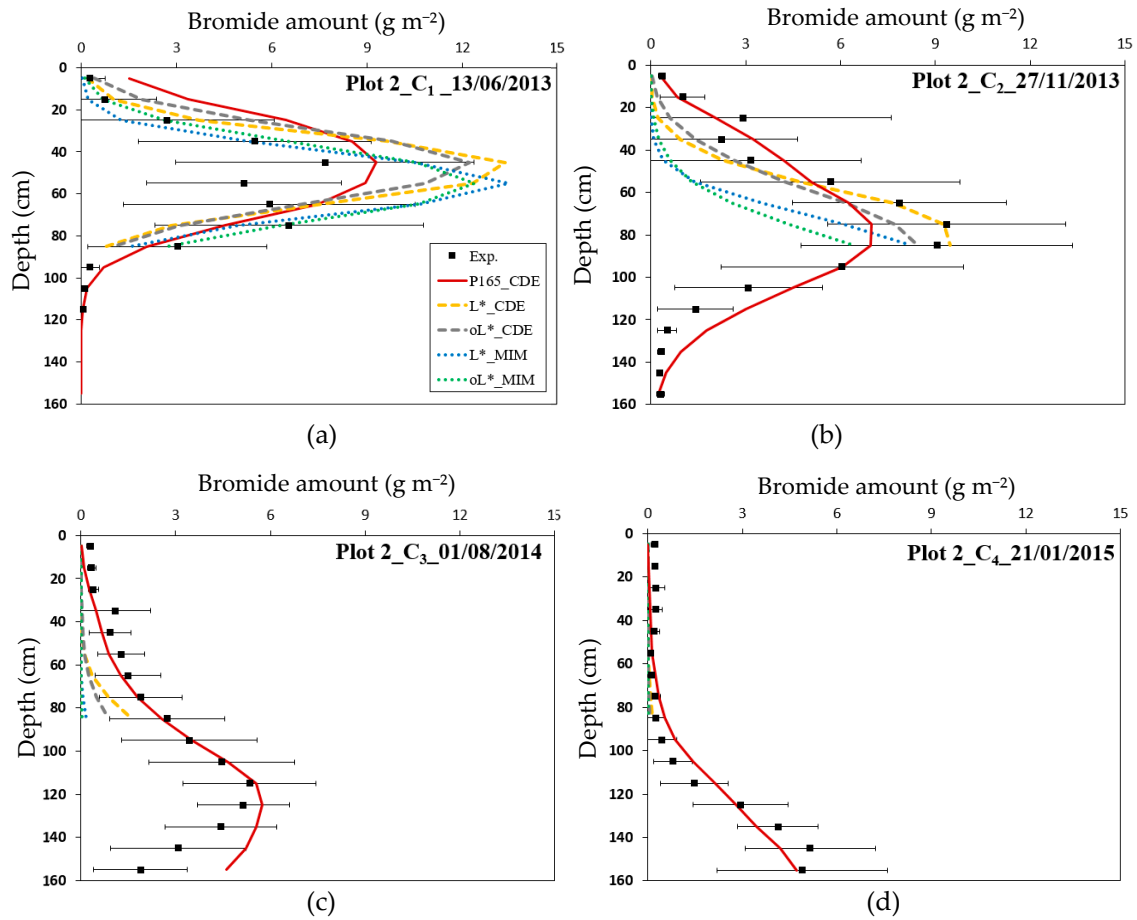


**Figure S8.** Comparison between experimental and simulated bromide concentrations in Field Plot 2 for the four monitoring campaigns (C1 (a), C2 (b), C3 (c), and C4 (d)).

Note: Each experimental point is the average of 8 to 11 samples and is accompanied by its standard deviation. P165\_CDE for results obtained with HYDRUS-1D with the convection-dispersion equation and parameters optimized on the 165 cm deep profile; L\*\_CDE for the results obtained with the convection-dispersion equation and by applying the mean optimized parameters from the six lysimeters; L\*\_MIM for the results obtained with the mobile-immobile model and by applying the mean optimized parameters from the six lysimeters; oL\*, the same as L\* but for saturated water content values ( $\theta_s^*$ ) again optimized for each soil material. Results obtained with the convection-dispersion equation and parameters optimized on the 90 cm deep profile are not shown since no significant differences were found with P165\_CDE for simulated bromide amount.

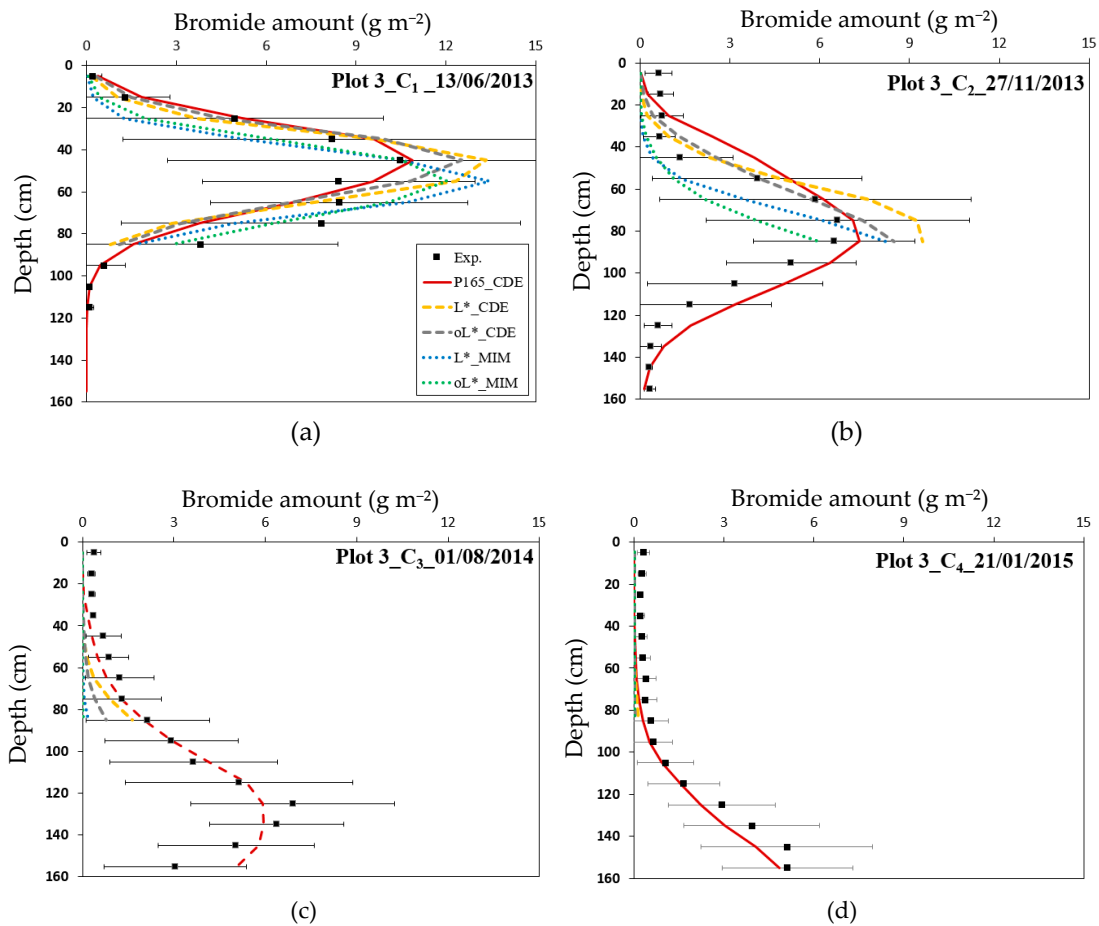


**Figure S8 (continued).** Comparison between experimental and simulated bromide concentrations in Field Plot 3 for the four monitoring campaigns (C<sub>1</sub> (a), C<sub>2</sub> (b), C<sub>3</sub> (c), and C<sub>4</sub> (d)).

Note: Each experimental point is the average of 8 to 11 samples and is accompanied by its standard deviation. P165\_CDE for results obtained with HYDRUS-1D with the convection-dispersion equation and parameters optimized on the 165 cm deep profile; L\*<sub>CDE</sub> for the results obtained with the convection-dispersion equation and by applying the mean optimized parameters from the six lysimeters; L\*<sub>MIM</sub> for the results obtained with the mobile-immobile model and by applying the mean optimized parameters from the six lysimeters; oL\*, the same as L\* but for saturated water content values ( $\theta_s^*$ ) again optimized for each soil material. Results obtained with the convection-dispersion equation and parameters optimized on the 90 cm deep profile are not shown since no significant differences were found with P165\_CDE for simulated bromide amount.

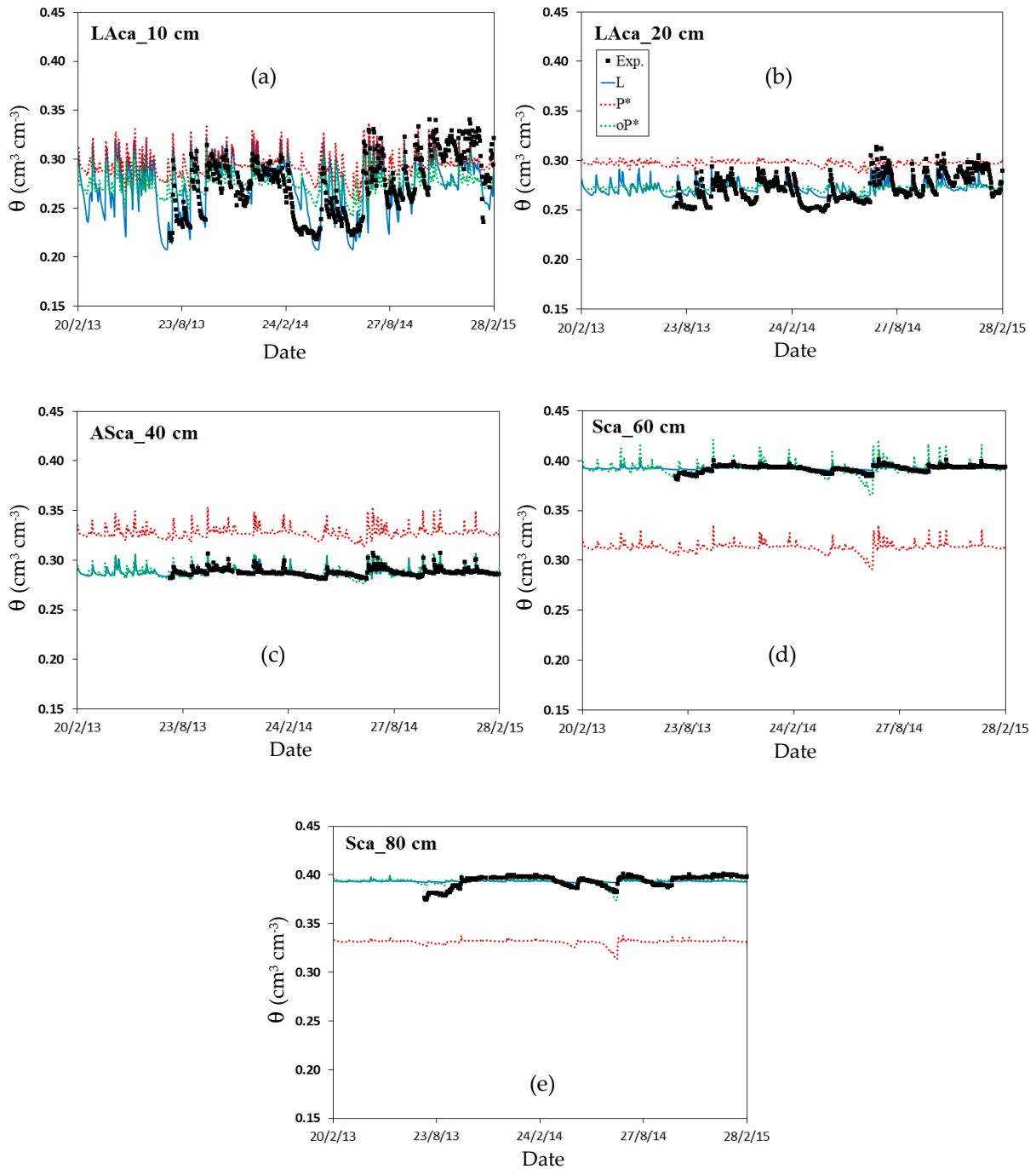


**Figure S9.** Comparison between experimental and simulated volumetric water content data at the 10 (a), 20 (b), 40 (c), 60 (d) and 80 (e) cm depths on Lys. 4.

Note: L for results obtained with the parameters optimized with HYDRUS-1D on lysimeter data; P\* for results obtained by applying the mean optimized parameters from the 165 cm deep profile of the three field plots; oP\*, the same as P\* but for saturated water content values ( $\theta_s^*$ ) again optimized for each soil material.

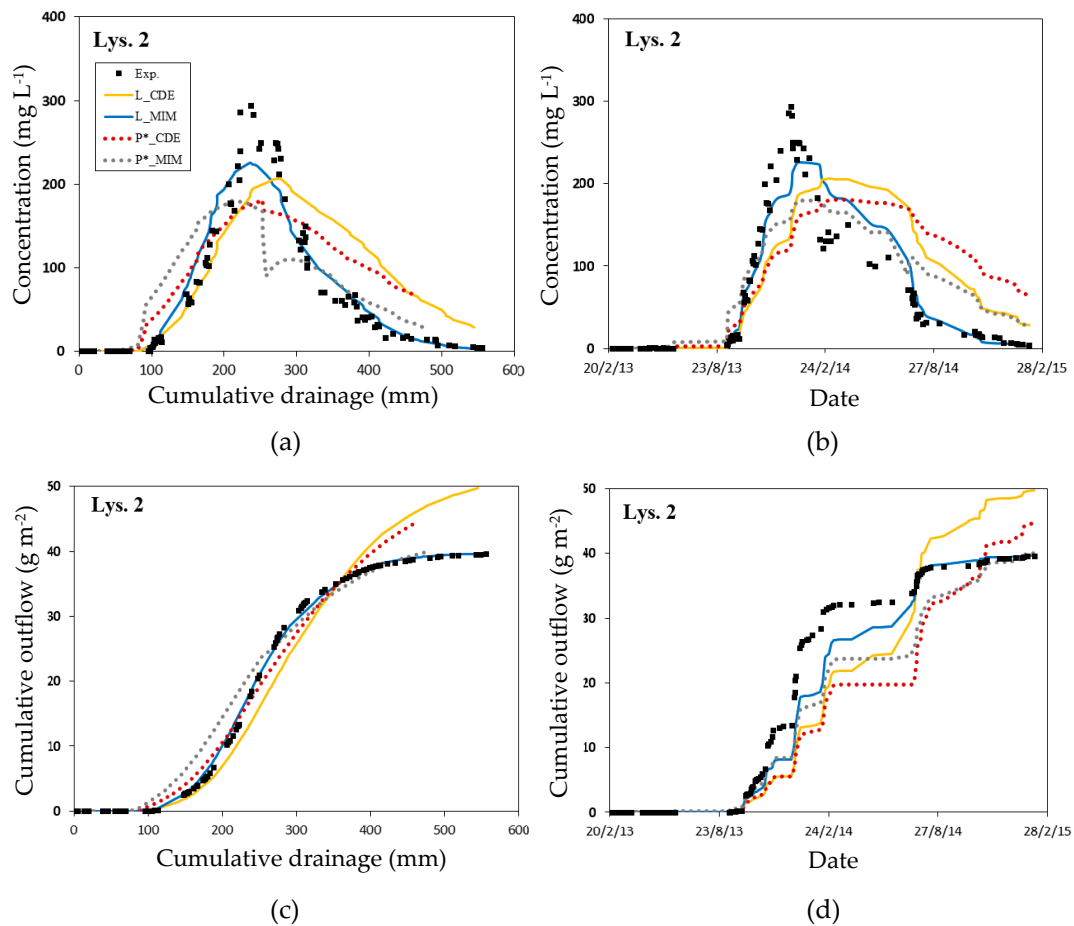


**Figure S10.** Comparison between experimental and simulated bromide concentration and cumulative outflow as a function of cumulative drainage ((a); (c)) and time ((b); (d)) on Lys. 2.

Note: L\_CDE for results obtained with the convection-dispersion equation and parameters optimized with HYDRUS-1D on lysimeter data; L\_MIM for results obtained with the mobile-immobile model and parameters optimized with HYDRUS-1D on lysimeter data; P\*\_CDE for results obtained with the convection-dispersion equation and by applying the mean optimized parameters from the 165 cm deep profiles of the three field plots; P\*\_MIM for the results obtained with the mobile-immobile model and by applying the mean optimized parameters from the 165 cm deep profiles of the three field plots. Results obtained with oP\* are not shown since the bromide concentration dynamics found as a function of cumulative drainage and time were similar to P\*.

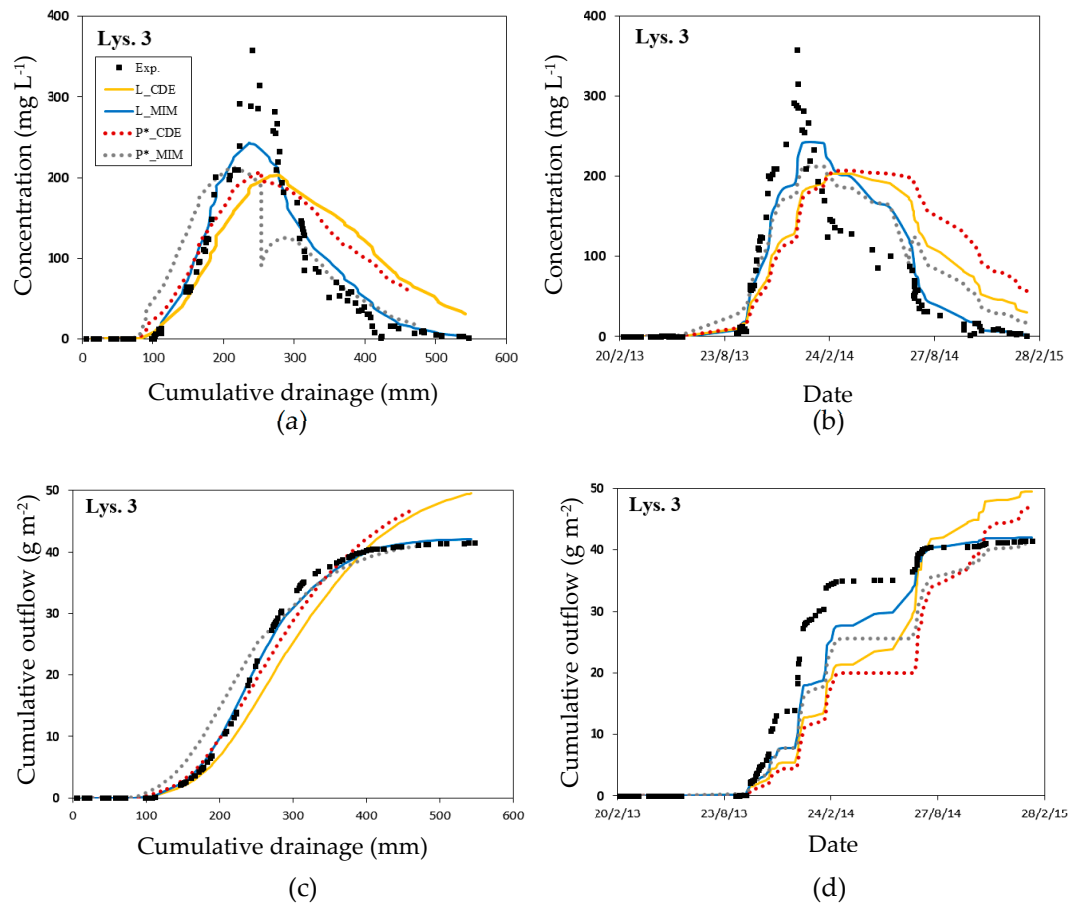


**Figure S10 (continued).** Comparison between experimental and simulated bromide concentration and cumulative outflow as a function of cumulative drainage ((a); (c)) and time ((b); (d)) on Lys. 3. Note: L\_CDE for results obtained with the convection-dispersion equation and parameters optimized with HYDRUS-1D on lysimeter data; L\_MIM for results obtained with the mobile-immobile model and parameters optimized with HYDRUS-1D on lysimeter data; P\*\_CDE for results obtained with the convection-dispersion equation and by applying the mean optimized parameters from the 165 cm deep profiles of the three field plots; P\*\_MIM for the results obtained with the mobile-immobile model and by applying the mean optimized parameters from the 165 cm deep profiles of the three field plots. Results obtained with oP\* are not shown since the bromide concentration dynamics found as a function of cumulative drainage and time were similar to P\*.

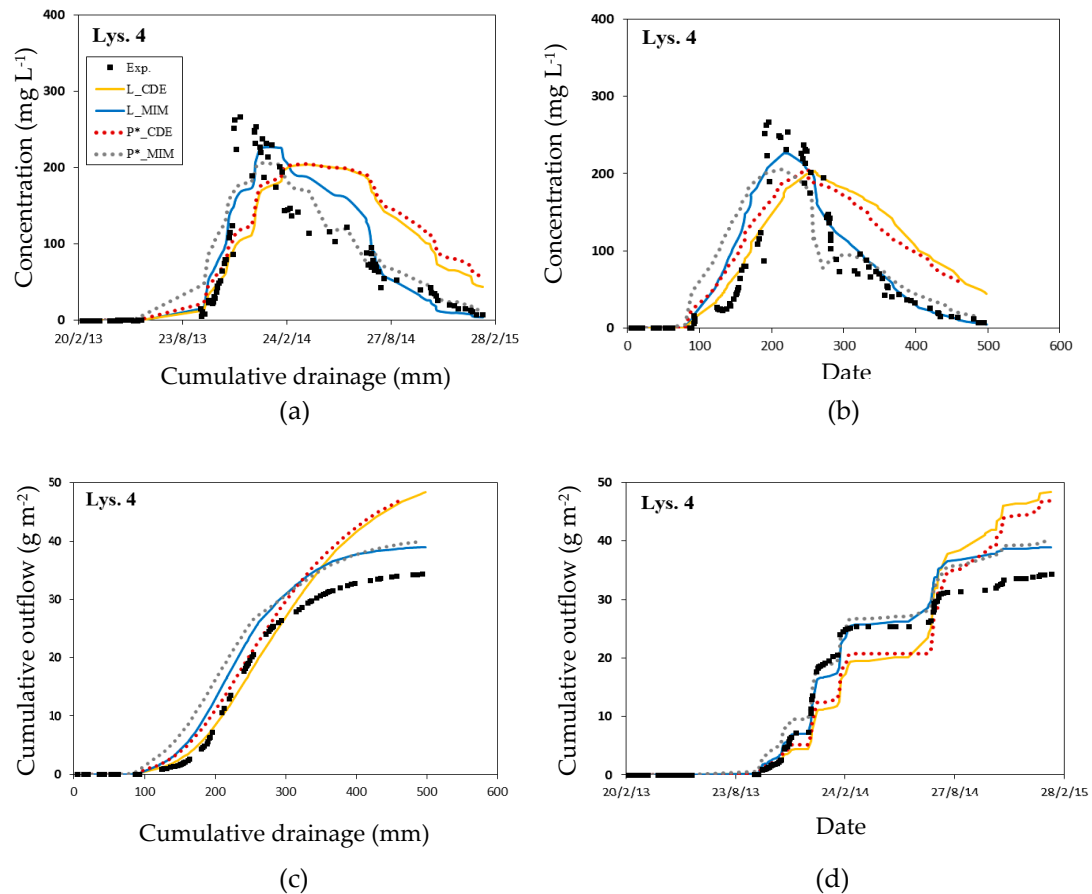


**Figure S10 (continued).** Comparison between experimental and simulated bromide concentration and cumulative outflow as a function of cumulative drainage ((a); (c)) and time ((b); (d)) on Lys. 4.

Note: L\_CDE for results obtained with the convection-dispersion equation and parameters optimized with HYDRUS-1D on lysimeter data; L\_MIM for results obtained with the mobile-immobile model and parameters optimized with HYDRUS-1D on lysimeter data; P\*\_CDE for results obtained with the convection-dispersion equation and by applying the mean optimized parameters from the 165 cm deep profiles of the three field plots; P\*\_MIM for the results obtained with the mobile-immobile model and by applying the mean optimized parameters from the 165 cm deep profiles of the three field plots. Results obtained with oP\* are not shown since the bromide concentration dynamics found as a function of cumulative drainage and time were similar to P\*.

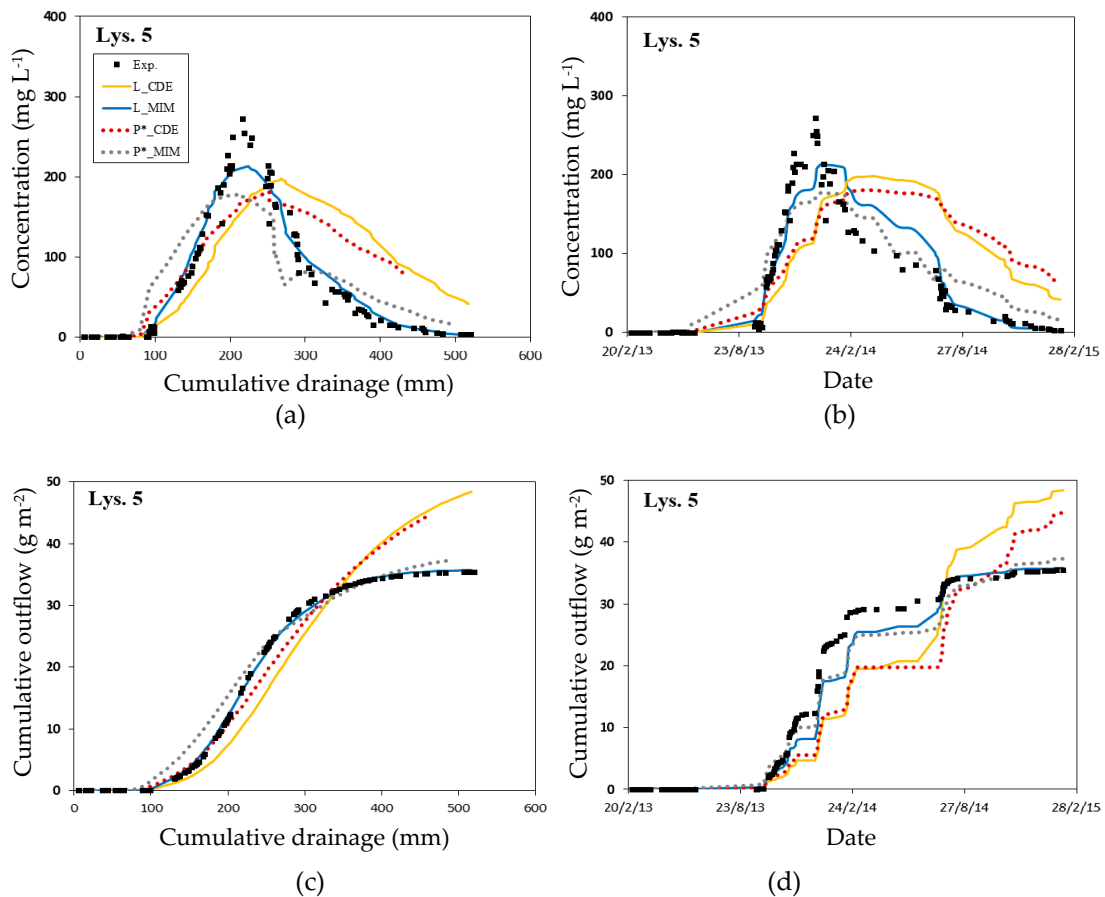


**Figure S10 (continued).** Comparison between experimental and simulated bromide concentration and cumulative outflow as a function of cumulative drainage ((a); (c)) and time ((b); (d)) on Lys. 5. Note: L\_CDE for results obtained with the convection-dispersion equation and parameters optimized with HYDRUS-1D on lysimeter data; L\_MIM for results obtained with the mobile-immobile model and parameters optimized with HYDRUS-1D on lysimeter data; P\*\_CDE for results obtained with the convection-dispersion equation and by applying the mean optimized parameters from the 165 cm deep profiles of the three field plots; P\*\_MIM for the results obtained with the mobile-immobile model and by applying the mean optimized parameters from the 165 cm deep profiles of the three field plots. Results obtained with oP\* are not shown since the bromide concentration dynamics found as a function of cumulative drainage and time were similar to P\*.



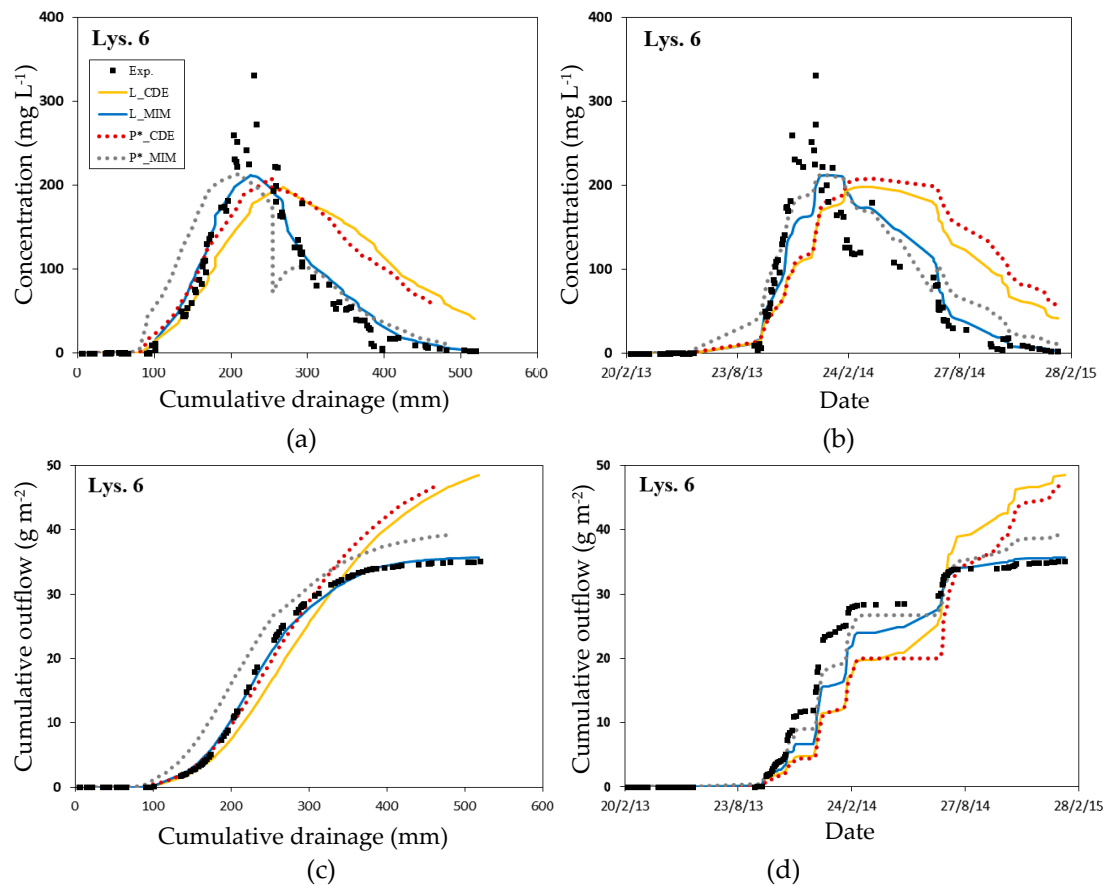


**Figure S10 (continued).** Comparison between experimental and simulated bromide concentration and cumulative outflow as a function of cumulative drainage ((a); (c)) and time ((b); (d)) on Lys. 6. Note: L\_CDE for results obtained with the convection-dispersion equation and parameters optimized with HYDRUS-1D on lysimeter data; L\_MIM for results obtained with the mobile-immobile model and parameters optimized with HYDRUS-1D on lysimeter data; P\*\_CDE for results obtained with the convection-dispersion equation and by applying the mean optimized parameters from the 165 cm deep profiles of the three field plots; P\*\_MIM for the results obtained with the mobile-immobile model and by applying the mean optimized parameters from the 165 cm deep profiles of the three field plots. Results obtained with oP\* are not shown since the bromide concentration dynamics found as a function of cumulative drainage and time were similar to P\*.

**Table S1.** Particle size fractions (in %) of the eight soil materials of the three field plots.

Soil Material	Field Plot 1			Field Plot 2			Field Plot 3		
	Clay	Silt	Sand	Clay	Silt	Sand	Clay	Silt	Sand
M <sub>1p</sub>	21.4 (0.5)	70.3 (1.2)	8.3 (1.3)	25.3 (0.5)	65.9 (1.2)	8.7 (0.6)	17.0 (0.4)	74.1 (0.9)	8.9 (0.6)
M <sub>2p</sub>	20.9 (0.8)	71.3 (0.9)	7.9 (0.6)	25.8 (0.2)	65.5 (0.3)	8.8 (0.4)	17.4 (0.6)	74.0 (0.9)	8.6 (0.6)
M <sub>3p</sub>	19.0 (1.7)	73.8 (3.1)	7.2 (1.4)	25.5 (1)	68.7 (1.5)	5.8 (0.4)	22.3 (1.8)	72.1 (2.4)	5.7 (0.6)
M <sub>4p</sub>	17.3 (0.3)	76.5 (1.2)	6.2 (0.9)	23.5 (1.8)	71.0 (1.8)	5.6 (0.3)	23.1 (1.8)	71.4 (2.7)	5.5 (0.5)
M <sub>5p</sub>	16.8 (0.4)	76.2 (1.7)	6.9 (1.0)	21.1 (0.9)	72.4 (1.8)	6.5 (1)	20.5 (2.5)	71.5 (4)	7.9 (5.5)
M <sub>6p</sub>	15.7 (1.5)	78.4 (5.7)	5.9 (1.7)	15.9 (2.8)	78.2 (4.6)	6.0 (1.8)	18.3 (1.3)	75.2 (6.2)	6.5 (5.3)
M <sub>7p</sub>	13.4 (0.4)	81.3 (1.7)	5.2 (1.7)	13.0 (0.5)	81.3 (2.7)	5.7 (2.8)	17.7 (1.4)	75.6 (4.1)	6.8 (3.2)
M <sub>8p</sub>	10.6 (5.6)	66.8 (14)	22.7 (18.2)	8.7 (4.1)	50.5 (21.8)	40.8 (26.9)	13.5 (0.9)	64.2 (6.1)	22.2 (6.9)

Note: Three samples were taken every 10 cm from 0 to 170 cm depth in each field plot. Means were calculated from the three values obtained at all depths included in those defining the soil material. Standard deviations are given in parentheses.

**Table S2.** Bulk density and saturated hydraulic conductivity mean values obtained at each instrumented depth in each field plot.

Depth. (cm)	$\rho_b$ (g cm <sup>-3</sup> )	$K_s$ (cm d <sup>-1</sup> )
10	1.32 (0.11)	110.2 (78.2)
20	1.38 (0.12)	575.2 (245.0)
37	1.33 (0.08)	71.0 (37.2)
50	1.22 (0.05)	76.9 (18.4)
65	1.28 (0.06)	29.1 (8.4)
90	1.41 (0.08)	16.7 (6.3)
120	1.45 (0.07)	16.1 (4.0)
165	1.57 (0.09)	19.8 (13.3)

Note: For  $K_s$ , three samples were taken at each instrumented depth of Field Plot 3. For  $\rho_b$ , six samples were taken below the surface layer (LAca) during instrumentation and 25 were taken at 10 and 20 cm depth at different times of the year and for different soil structural state. Standard deviations are given in parentheses.

**Table S3.** Parameters optimized using HYDRUS-1D for each of the eight soil materials of Field Plot 2.

Soil Material	$\theta_r$ ( $\text{cm}^3 \text{cm}^{-3}$ )	$\theta_s$ ( $\text{cm}^3 \text{cm}^{-3}$ )	$\alpha$ ( $\text{cm}^{-1}$ )	$n$ (-)	$K_s$ ( $\text{cm d}^{-1}$ )	$\lambda$ (cm)	$\theta_s^*$ ( $\text{cm}^3 \text{cm}^{-3}$ )
M <sub>1p</sub>	0.062 (0.075) [0.062–0.108]	<b>0.355</b> (0.382) [0.350–0.360]	0.019 (0.047) [0.018–0.020]	<b>1.199</b> (1.160) [1.187–1.210]	41.8 [37.0–46.7]	3.0	0.342 [0.340–0.344]
M <sub>2p</sub>	0.079 (0.085) [0.077–0.097]	<b>0.393</b> (0.373) [0.378–0.409]	0.022 (0.050) [0.014–0.031]	<b>1.211</b> (1.163) [1.187–1.233]	575.2	3.0	0.344 [0.341–0.347]
M <sub>3p</sub>	0.109 (0.103) [0.095–0.109]	<b>0.333</b> (0.389) [0.325–0.341]	0.031 (0.044) [0.028–0.034]	<b>1.103</b> (1.165) [1.087–1.119]	69.7	6.0	0.334 [0.332–0.336]
M <sub>4p</sub>	0.082 (0.086) [0.082–0.095]	<b>0.352</b> (0.418) [0.349–0.355]	0.037 (0.073) [0.035–0.039]	1.179 (1.187) [1.146–1.212]	73.9 [58.6–89.1]	6.0	0.309 [0.307–0.311]
M <sub>5p</sub>	0.044 (0.049) [0.044–0.054]	0.392 (0.387) [0.385–0.399]	0.012 (0.013) [0.012–0.012]	<b>1.437</b> (1.254) [1.374–1.504]	<b>16.5</b> [16.2–16.8]	2.5	0.313 [0.311–0.315]
M <sub>6p</sub>	0.044 (0.046) [0.043–0.051]	<b>0.352</b> (0.379) [0.347–0.357]	0.006 (0.007) [0.006–0.007]	<b>1.781</b> (1.315) [1.673–1.889]	16.7	2.5	0.313 [0.311–0.315]
M <sub>7p</sub>	0.049 (0.050) [0.049–0.053]	<b>0.349</b> (0.387) [0.343–0.356]	0.002 (0.003) [0.002–0.003]	<i>1.547</i> (1.547)	16.1	4.0	/
M <sub>8p</sub>	0.036 (0.027) [0.024–0.036]	<b>0.374</b> (0.293) [0.369–0.379]	0.005 (0.005) [0.004–0.006]	<i>1.365</i> (1.365)	19.8	4.0	/

Note: Initial values obtained with RetC from laboratory water retention measurements are given in parentheses after the optimized value. Confidence intervals associated with parameters optimized using HYDRUS-1D are given in brackets. Parameters  $\theta_r$ ,  $\theta_s$ ,  $\alpha$ ,  $n$  and  $K_s$  optimized using HYDRUS-1D are highlighted: (i) in **bold** for parameters whose **optimized value is not included in the initial bounds**, (ii) in *italics* for non-optimized parameters *set to the mean initial value*. Saturated water content values re-optimized during the cross-simulations are noted  $\theta_s^*$ . The soil dispersivity ( $\lambda$ ) was set manually for each individual soil material.

**Table S3 (continued).** Parameters optimized using HYDRUS-1D for each of the eight soil materials of Field Plot 3.

Soil Material.	$\theta_r$ ( $\text{cm}^3 \text{cm}^{-3}$ )	$\theta_s$ ( $\text{cm}^3 \text{cm}^{-3}$ )	$\alpha$ ( $\text{cm}^{-1}$ )	$n$ (-)	$K_s$ ( $\text{cm d}^{-1}$ )	$\lambda$ (cm)	$\theta_s^*$ ( $\text{cm}^3 \text{cm}^{-3}$ )
M <sub>1p</sub>	0.065 (0.068) [0.065–0.070]	<b>0.347</b> (0.413) [0.343–0.351]	<b>0.018</b> (0.042) [0.018–0.019]	<b>1.239</b> (1.181) [1.227–1.250]	<b>26.8</b> [17.2–35.9]	1.0	0.327 [0.325–0.328]
M <sub>2p</sub>	0.069 (0.073) [0.069–0.080]	<b>0.304</b> (0.369) [0.302–0.306]	0.002 (0.004) [0.002–0.003]	<b>1.317</b> (1.202) [1.226–1.409]	<i>575.2</i>	1.0	0.318 [0.317–0.320]
M <sub>3p</sub>	0.077 (0.074) [0.071–0.077]	<b>0.362</b> (0.435) [0.360–0.364]	0.058 (0.055) [0.054–0.061]	<b>1.089</b> (1.174) [1.080–1.099]	<b>508.6</b> [407.9–609.3]	3.0	0.350 [0.349–0.352]
M <sub>4p</sub>	0.070 (0.072) [0.070–0.075]	<b>0.332</b> (0.426) [0.330–0.334]	0.046 (0.054) [0.042–0.049]	<b>1.103</b> (1.172) [1.088–1.118]	<b>147.3</b> [105.0–189.7]	3.0	0.318 [0.316–0.319]
M <sub>5p</sub>	0.052 (0.054) [0.052–0.058]	<b>0.340</b> (0.419) [0.334–0.345]	<b>0.018</b> (0.045) [0.016–0.020]	1.224 (1.206) [1.187–1.260]	29.0 [10.7–46.9]	2.0	0.303 [0.301–0.304]
M <sub>6p</sub>	0.043 (0.047) [0.043–0.052]	<b>0.340</b> (0.370) [0.334–0.346]	0.011 (0.012) [0.009–0.012]	1.226 (1.251) [1.187–1.265]	<i>16.7</i>	2.0	0.318 [0.317–0.320]
M <sub>7p</sub>	0.041 (0.048) [0.041–0.053]	<b>0.349</b> (0.400) [0.343–0.355]	<b>0.002</b> (0.005) [0.002–0.002]	<i>1.439</i> (1.439)	<i>16.1</i>	2.0	/
M <sub>8p</sub>	0.041 (0.045) [0.041–0.053]	<b>0.391</b> (0.361) [0.376–0.407]	<b>0.006</b> (0.003) [0.003–0.010]	1.524 (1.471) [1.118–1.931]	<i>19.8</i>	2.0	/

Note: Initial values obtained with RetC from laboratory water retention measurements are given in parentheses after the optimized value. Confidence intervals associated with parameters optimized using HYDRUS-1D are given in brackets. Parameters  $\theta_r$ ,  $\theta_s$ ,  $\alpha$ ,  $n$  and  $K_s$  optimized using HYDRUS-1D are highlighted: (i) in **bold** for parameters whose **optimized value is not included in the initial bounds**, (ii) in *italics* for non-optimized parameters *set to the mean initial value*. Saturated water content values re-optimized during the cross-simulations are noted  $\theta_s^*$ . The soil dispersivity ( $\lambda$ ) was set manually for each individual soil material.

**Table S4.** Efficiency coefficients calculated at each instrumented depth in Field Plots 2 and 3 and based on different optimization procedures using HYDRUS-1D.

<b>Field Plot 2</b>	<b>M<sub>1p_10</sub></b>	<b>M<sub>2p_20</sub></b>	<b>M<sub>3p_37</sub></b>	<b>M<sub>4p_50</sub></b>	<b>M<sub>5p_65</sub></b>	<b>M<sub>6p_90</sub></b>	<b>M<sub>7p_120</sub></b>	<b>M<sub>8p_165</sub></b>
h_RP165	0.44	0.51	0.39	0.38	0.78	0.84	0.85	1.00
h_P165	0.53	0.65	0.69	0.57	0.74	0.83	0.85	1.00
h_P90	0.52	0.66	0.72	0.73	0.88	1.00	/	/
h_L*	0.46	0.64	0.52	0.60	0.84	1.00	/	/
h_oL*	0.53	0.62	0.54	0.63	0.84	1.00	/	/
θ_RP165	0.21	0.48	-0.45	-5.24	-3.87	-7.71	-33.12	-54.70
θ_P165	0.46	0.69	0.50	0.63	0.82	0.88	0.74	0.82
θ_P90	0.47	0.70	0.55	0.74	0.72	0.55	/	/
θ_L*	-0.50	-0.62	-0.25	-9.06	-28.42	-25.57	/	/
θ_oL*	0.40	0.31	0.42	0.50	0.54	0.55	/	/

<b>Field Plot 3</b>	<b>M<sub>1p_10</sub></b>	<b>M<sub>2p_20</sub></b>	<b>M<sub>3p_37</sub></b>	<b>M<sub>4p_50</sub></b>	<b>M<sub>5p_65</sub></b>	<b>M<sub>6p_90</sub></b>	<b>M<sub>7p_120</sub></b>	<b>M<sub>8p_165</sub></b>
h_RP165	0.46	0.41	0.29	0.09	0.34	0.76	0.77	1.00
h_P165	0.63	0.68	0.76	0.72	0.79	0.86	0.80	1.00
h_P90	0.64	0.69	0.76	0.80	0.85	1.00	/	/
h_L*	0.12	0.64	0.49	0.64	0.73	1.00	/	/
h_oL*	0.29	0.63	0.50	0.66	0.73	1.00	/	/
θ_RP165	-1.85	-8.63	-6.92	-22.11	-9.83	-2.58	-23.09	-0.04
θ_P165	0.45	0.36	0.54	0.61	0.70	0.85	0.72	0.91
θ_P90	0.46	0.37	0.56	0.67	0.75	0.73	/	/
θ_L*	-0.15	-0.69	0.44	-6.11	-44.23	-71.89	/	/
θ_oL*	0.38	0.30	0.50	0.52	0.57	0.78	/	/

Note: RP165 for results obtained with the parameters optimized with RetC, P165 for results obtained with the parameters optimized with HYDRUS-1D on the 165 cm deep profile; P90 for results obtained by applying the parameters optimized for the 165 cm deep profile to the 90 cm deep profile; L\* for results obtained by applying the mean optimized parameters from the six lysimeters; oL\*, the same as L\* but for saturated water content values ( $\theta_s^*$ ) again optimized for each soil material.

**Table S5.** Efficiency coefficients calculated for bromide transport for each monitoring campaign (C<sub>1</sub> to C<sub>4</sub>) conducted on Field Plots 2 and 3 and based on different optimization procedures using HYDRUS-1D.

	C <sub>1</sub> (13 June 2013)	C <sub>2</sub> (27 November 2013)	C <sub>3</sub> (01 August 2014)	C <sub>4</sub> (21 January 2015)
Field Plot 2				
P165_CDE	0.53	0.86	0.68	0.95
P90_CDE	−0.03	0.86	0.83	/
L*_CDE	−1.29	0.88	−0.39	/
oL*_CDE	−0.79	0.84	−1.02	/
L*_MIM	−0.98	0.27	−2.09	/
oL*_MIM	−0.56	−0.03	−2.26	/
Field Plot 3				
P165_CDE	0.88	0.77	0.91	0.94
P90_CDE	0.74	0.77	0.73	/
L*_CDE	0.39	0.63	0.18	/
oL*_CDE	0.56	0.86	−0.68	/
L*_MIM	0.36	0.70	−1.75	/
oL*_MIM	0.67	0.47	−2.01	/

Note: P165 for results obtained with the parameters optimized with HYDRUS-1D on the 165 cm deep profile; P90 for results obtained by applying the parameters optimized for the 165 cm deep profile to the 90 cm deep profile; L\* for results obtained by applying the mean optimized parameters from the six lysimeters; oL\*, the same as L\* but for saturated water content values ( $\theta_s^*$ ) again optimized for each soil material. CDE for results obtained with the convection-dispersion equation. MIM for results obtained with the mobile-immobile model. Due to a lack of bromide in the 90 cm deep profile, efficiency coefficients were not calculated for the fourth monitoring campaign.

**Table S6.** Efficiency coefficients calculated for water content data at each depth instrumented in Lys. 4 using HYDRUS-1D.

	<b>M<sub>1c_10</sub></b>	<b>M<sub>2c_20</sub></b>	<b>M<sub>3c_40</sub></b>	<b>M<sub>4c_60</sub></b>	<b>M<sub>5c_80</sub></b>
$\theta\_L$	0.54	0.41	0.22	0.18	0.09
$\theta\_P^*$	-0.42	-1.65	-71.12	-495.07	-103.90
$\theta\_oP^*$	0.25	0.26	-0.01	-0.66	0.34

Note: L for results obtained with the parameters optimized with HYDRUS-1D on lysimeter data; P\* for results obtained by applying the mean optimized parameters from 165 cm deep profile of the three field plots; oP\*, the same as P\* but for saturated water content values ( $\theta_s^*$ ) again optimized for each soil material.

**Table S7.** Efficiency coefficients calculated for daily drainage data on Lys. 2, 3, 4, 5 and 6 using HYDRUS-1D.

	<b>Lys. 2</b>	<b>Lys. 3</b>	<b>Lys. 4</b>	<b>Lys. 5</b>	<b>Lys. 6</b>
d_L	0.85	0.80	0.77	0.78	0.72
CV	-2.3	-1.1	0.6	-1.0	-0.9
d_P*	0.82	0.82	0.82	0.81	0.80
CV	-16.7	-15.4	-6.2	-11.1	-10.9
d_oP*	0.82	0.82	0.81	0.81	0.79
CV	-16.9	-15.6	-6.3	-11.2	-11

Note: L for results obtained with the parameters optimized with HYDRUS-1D on lysimeter data; P\* for results obtained by applying the mean optimized parameters from 165 cm deep profile of the three field plots; oP\*, the same as P\* but for saturated water content values ( $\theta_s^*$ ) again optimized for each soil material. Coefficients of variation (CV) were calculated from cumulative experimental and simulated drainage data and are given in %.



**Table S8.** Parameters optimized using HYDRUS-1D for each of the six soil materials of Lys. 2, 3, 4, 5 and 6.

Soil Material	$\theta_s$	$K_s$	$\theta_s$	$K_s$	$\theta_s$	$K_s$	$\theta_s$	$K_s$	$\theta_s$	$K_s$
	Lys. 2		Lys. 3		Lys. 4		Lys. 5		Lys. 6	
M <sub>1c</sub>	0.289	10.0	0.289	10.0	<b>0.324</b> (0.324) [0.322–0.325] {0.322–0.325}	<b>31.2</b> [27.6–34.7]	0.291	20.5	0.293	20
M <sub>2c</sub>	0.288	1000.0	0.288	1000	<b>0.298</b> (0.334) [0.297–0.299] {0.332–0.336}	<b>2067.2</b> [1839.0–2295.4]	0.298	1411.9	0.298	1500.0
M <sub>3c</sub>	0.307	44.9	0.307	44.9	<b>0.307</b> (0.320) [0.306–0.308] {0.318–0.321}	44.9 [38.1–51.6]	0.307	44.9	0.366	27.5
M <sub>4c</sub>	0.389	199.3	0.389	32.4	<b>0.407</b> (0.428) [0.406–0.408] {0.426–0.429}	<b>199.3</b> [71.4–328.6]	0.407	199.3	0.407	100
M <sub>5c</sub>	0.399	25	0.396	24.9	0.399 (0.400) [0.398–0.400] {0.399–0.402}	<b>10.0</b>	0.396	25	0.396	17.5

Note: Initial parameters are given in parentheses after the optimized value. Confidence intervals associated with parameters optimized using HYDRUS-1D are given in brackets. Parameters  $\theta_r$ ,  $\theta_s$ ,  $\alpha$ ,  $n$  and  $K_s$  optimized using HYDRUS-1D are highlighted: (i) in **bold** for parameters whose **set value is not included in the initial bounds**, (ii) in *italics* for parameters *that were set manually*. Saturated water content values re-optimized during the cross simulations ( $\theta_s^*$ ) are given in parentheses after the optimized value of  $\theta_s$  and confidence intervals associated with  $\theta_s^*$  are given in braces.

**Table S9.** Values of dispersivity, immobile water content and mass exchange coefficient parameters manually set using HYDRUS-1D for all soil materials of Lys. 2, 3, 4, 5 and 6.

	<b>Lys. 2</b>	<b>Lys. 3</b>	<b>Lys. 4</b>	<b>Lys. 5</b>	<b>Lys. 6</b>
$\lambda$ (cm)	1.00	0.75	1.00	1.00	0.75
$\theta_{im}$ (cm <sup>3</sup> cm <sup>-3</sup> )	0.065	0.065	0.075	0.090	0.080
$C_0^*$ (g m <sup>-2</sup> )	50.7	53.9	50.0	51.8	49.1
$\alpha_{ph}$ (d <sup>-1</sup> )	10 <sup>-6</sup>	10 <sup>-6</sup>	10 <sup>-6</sup>	10 <sup>-6</sup>	10 <sup>-6</sup>

Note: Initial amounts of bromide manually re-optimized are noted  $C_0^*$ .

**Table S10.** Efficiency coefficients calculated for bromide concentration and cumulated outflow as a function of time (and cumulative drainage in parentheses) from Lys. 2, 3, 4, 5 and 6 and based on different optimization procedures using HYDRUS-1D.

		Lys. 2	Lys. 3	Lys. 4	Lys. 5	Lys. 6
Concentration	L_CDE	0.51 (0.69)	0.47 (0.63)	0.48 (0.58)	0.27 (0.44)	0.33 (0.46)
	L_MIM	0.89 (0.93)	0.83 (0.93)	0.84 (0.85)	0.90 (0.96)	0.83 (0.93)
	P*_CDE	0.35 (0.74)	0.34 (0.71)	0.52 (0.66)	0.29 (0.67)	0.32 (0.65)
	P*_MIM	0.82 (0.55)	0.79 (0.53)	0.75 (0.64)	0.83 (0.82)	0.80 (0.69)
Cumulated Outflow	L_CDE	0.16 (0.10)	0.24 (0.05)	0.45 (-0.41)	0.01 (-0.42)	-0.27 (-0.08)
	L_MIM	0.54 (0.64)	0.63 (0.45)	0.78 (0.20)	0.67 (0.45)	0.59 (0.65)
	P*_CDE	0.15 (0.62)	0.20 (0.49)	0.46 (-0.05)	0.12 (-0.20)	0.06 (0.36)
	P*_MIM	0.55 (0.64)	0.59 (0.48)	0.71 (0.29)	0.58 (0.06)	0.64 (0.16)

Note: L\_CDE for results obtained with the convection-dispersion equation and parameters optimized with HYDRUS-1D on lysimeter data; L\_MIM for results obtained with the mobile-immobile model and parameters optimized with HYDRUS-1D on lysimeter data; P\*\_CDE for results obtained with the convection-dispersion equation and by applying the mean optimized parameters from the 165 cm deep profiles of the three field plots; P\*\_MIM for the results obtained with the mobile-immobile model and by applying the mean optimized parameters from the 165 cm deep profiles of the three field plots.

**Table S11.** Mean values of the parameters optimized using HYDRUS-1D on the lysimeter data used for cross simulations on field plot data.

Layer	Soil Material	$\theta_r$ ( $\text{cm}^3 \text{ cm}^{-3}$ )	$\theta_s$ ( $\text{cm}^3 \text{ cm}^{-3}$ )	$\alpha$ ( $\text{cm}^{-1}$ )	$n$ (-)	$K_s$ ( $\text{cm d}^{-1}$ )
LAca	M <sub>1c</sub>	0.062	0.294	0.020	1.194	17.1
	M <sub>2c</sub>	0.097	0.293	0.200	1.050	1134.8
ASca	M <sub>3c</sub>	0.109	0.353	0.035	1.100	123.7
Sca	M <sub>4c</sub>	0.065	0.403	0.012	1.140	150.4
	M <sub>5c</sub>	0.058	0.398	0.009	1.150	61.2

Note: To take into account the characteristics of the soil materials defining the soil profiles of the field plots and lysimeters, the parameters obtained for M<sub>1c</sub>, M<sub>2c</sub>, M<sub>4c</sub> and M<sub>5c</sub> were respectively applied to M<sub>1p</sub>, M<sub>2p</sub>, M<sub>5p</sub> and M<sub>6p</sub>. Parameters obtained for M<sub>3c</sub> were applied to M<sub>3p</sub> and M<sub>4p</sub>.

**Table S12.** Mean values of the parameters optimized on the three field plots using HYDRUS-1D for cross simulations on lysimeter data.

Layer	Soil Material	$\theta_r$ ( $\text{cm}^3 \text{cm}^{-3}$ )	$\theta_s$ ( $\text{cm}^3 \text{cm}^{-3}$ )	$\alpha$ ( $\text{cm}^{-1}$ )	$n$ (-)	$K_s$ ( $\text{cm d}^{-1}$ )	$\lambda$ ( $\text{cm}$ )
LAca	M <sub>1p</sub>	0.064	0.355	0.020	1.230	56.6	2.7
	M <sub>2p</sub>	0.075	0.359	0.034	1.224	642.4	2.7
ASca	M <sub>3p</sub>	0.087	0.356	0.041	1.125	207.9	4.3
	M <sub>4p</sub>	0.072	0.332	0.030	1.215	99.3	4.3
Sca	M <sub>5p</sub>	0.047	0.351	0.016	1.273	24.2	2.0
	M <sub>6p</sub>	0.045	0.340	0.007	1.554	16.7	2.0

Note: To take into account the characteristics of the soil materials defining the soil profiles of the field plots and lysimeters, the parameters obtained for M<sub>1p</sub>, M<sub>2p</sub>, M<sub>3p</sub>, M<sub>5p</sub> and M<sub>6p</sub> were respectively applied to M<sub>1c</sub>, M<sub>2c</sub>, M<sub>3c</sub>, M<sub>4c</sub> and M<sub>5c</sub>.



© 2019 by the authors. Submitted for possible open access publication under the terms and conditions of the Creative Commons Attribution (CC BY) license (<http://creativecommons.org/licenses/by/4.0/>).